Neutron Diffraction Study on the Structure of Liquid Cs-Sb Alloys

P. Lamparter, W. Martin, and S. Steeb
Max-Planck-Institut für Metallforschung, Institut für Werkstoffwissenschaften, Stuttgart

W. Freyland
Institut für Physikalische Chemie der Universität Marburg

Z. Naturforsch. **38 a**, 329–335 (1983); received November 11, 1982

By neutron diffraction experiments the total structure factors and the total pair correlation functions of liquid Cs-Sb alloys containing 85, 75, 65, and 50 at% Cs, respectively, were determined. The structural results confirm the non metallic properties of Cs-Sb melts.

The correspondence of the nearest neighbour atomic arrangement in liquid $Cs_{75}Sb_{25}$ and in the solid compound semiconductor Cs_3Sb suggests a similar type of bonding, namely by valence bonds and ionic forces simultaneously. The stability of this compound in the molten state leads to a microsegregation tendency between compound forming regions and excess Cs in the concentration range from pure Cs up to 25 at% Sb, which is established by a small angle scattering effect.

Proceeding from $Cs_{75}Sb_{25}$ to $Cs_{50}Sb_{50}$, a continuous change in the structure takes place. Covalently bonded Sb chains are formed just as found in the corresponding solid compounds ASb (A = alkali metal). An additional diffraction peak in front of the main peak of the structure factors within this composition range implies the formation of rather large molecular clusters in the alloys.

Introduction

A number of liquid alloy systems formed from metallic constituents is known, which exhibit non metallic properties near certain stoichiometric compositions. In liquid $Au_{50}Cs_{50}$ [1], $Li_{80}Pb_{20}$ [2], and $Mg_{66.7}Bi_{33.3}$ [3] e.g. the electrical conductivity drops by orders of magnitude compared to that of the pure elements. This metal-non metal transition clearly requires a change in the bonding characteristics to occur in these concentration ranges. In the last few years the nature of the chemical bonding in such semiconducting alloys was the subject of various experimental and theoretical studies (see e.g. [4–6]), emphasizing the question whether it is ionic due to charge transfer between the components or whether it is covalent and thus forming molecular units in the alloy.

For the case of the Au-Cs system evidence for predominantly ionic bonding has been given by a variety of investigations [1, 5, 7–10]. Concerning the Cs-Sb system, however, which exhibits a steep metal-non metal transition at the stoichiometric composition Cs_3Sb, from recent investigations of the electronic properties it was concluded that liquid Cs-Sb alloys are not essentially ionic, but that also covalent bonding takes place [7, 11].

The aim of the present study was to obtain information on the type of bonding in liquid Cs-Sb alloys by investigation of the atomic scale structure by means of neutron diffraction experiments. Even though from a diffraction experiment the nature of the chemical bonding obviously cannot be seen directly, this is closely related to the atomic structure of a liquid alloy.

Reprint requests to Prof. Dr. S. Steeb, MPI für Metallforschung, Institut für Werkstoffwissenschaften, Seestraße 92, 7000 Stuttgart 1.

Basic equations

In the following, a summary of the relations used in the present study will be given. For a comprehensive review see e.g. [12]. According to the Faber Ziman definition [13] the total structure factor $S^{FZ}(Q)$ is obtained from the coherently scattered intensity per atom $I_C(Q)$:

$$S^{FZ}(Q) = \frac{I_C(Q) - [\langle b^2\rangle - \langle b\rangle^2]}{\langle b\rangle^2}, \qquad (1)$$

where

Q = $(4\pi \sin\Theta)/\lambda$,
2Θ = scattering angle,
λ = wavelength,

0340-4811 / 83 / 0300-0329 $ 01.3 0/0. – Please order a reprint rather than making your own copy.

$\langle b \rangle = c_A b_A + c_B b_B$,
$\langle b^2 \rangle = c_A b_A^2 + c_B b_B^2$,
c_A, c_B = atomic concentrations of the components A and B,
b_A, b_B = coherent neutron scattering lengths of A and B.

From the structure factor the total pair correlation function $G(R)$ and the total pair density distribution function $\varrho(R)$ are calculated by Fourier transformation:

$$G(R) = 4\pi R[\varrho(R) - \varrho_0] = \frac{2}{\pi} \int_0^\infty Q[S^{FZ}(Q) - 1] \cdot \sin(Q R)\, dQ , \quad (2)$$

where

R = atomic pair distance,
ϱ_0 = mean atomic number density.

In a real experiment the integration range of (2) is given by the accessible 2Θ range.

For the case of a binary system the total $\varrho(R)$ function is a weighted sum of three partial pair density distribution functions $\varrho_{ij}(R)$:

$$\varrho(R) = \frac{c_A b_A^2}{\langle b \rangle^2} \varrho_{AA}(R) + \frac{c_B b_B^2}{\langle b \rangle^2} \varrho_{BB}(R) + \frac{2 c_A b_A b_B}{\langle b \rangle^2} \varrho_{AB}(R) . \quad (3)$$

$\varrho_{ij}(R)$ represents the number of j type atoms per unit volume at distance R from an i type atom. The so called total coordination number in the n-th shell around a reference atom is obtained according to (4):

$$N^n = \int_{R_1^n}^{R_0^n} 4\pi R^2 \varrho(R)\, dR . \quad (4)$$

It should be noted that the physical meaning of N^n is restricted because the choice of the integration limits which define the inner (R_1^n) and the outer (R_0^n) limit of the n-th shell is not unique. Furthermore besides c_i and $\varrho_{ij}(R)$ also the scattering lengths b_i enter into the value of N^n, which therefore depends on the kind of radiation used.

Inserting the partial pair density $\varrho_{ij}(R)$ into (4) one obtains the partial coordination number Z_{ij}^n of j type atoms in the n-th shell around an i type atom.

An alternative description of the structure of a binary alloy is given by the correlations between density- and concentration-fluctuations in terms of the three partial Bhatia Thornton structure factors $S_{NN}(Q)$, $S_{CC}(Q)$, and $S_{NC}(Q)$ and their Fourier transforms [14]. Hereby another definition of the total structure factor than that given in (1) is convenient:

$$S^{BT}(Q) = I_C(Q)/\langle b^2 \rangle . \quad (5)$$

$S^{BT}(Q)$ is related to the partials by (6):

$$S^{BT}(Q) = \frac{\langle b \rangle^2}{\langle b^2 \rangle} S_{NN}(Q) + \frac{(b_A - b_B)^2}{\langle b^2 \rangle} S_{CC}(Q) + \frac{2\langle b \rangle (b_A - b_B)}{\langle b^2 \rangle} S_{NC}(Q) . \quad (6)$$

$S_{NN}(Q)$ describes the correlations between number density fluctuations, $S_{CC}(Q)$ those between concentration fluctuations, and $S_{NC}(Q)$ the cross correlations which are present for the case of different atomic sizes in the binary alloy.

It should be noticed that the second and the third term in (6) vanish if both kinds of atoms have the same scattering length. That means that concentration fluctuations $S_{CC}(Q)$ do not contribute explicitely to the total scattering, but only implicitely to $S_{NN}(Q)$ via the cross correlations $S_{NC}(Q)$. This can easily be seen from the thermodynamic limit of (6) ($Q = 0$), for $b_A = b_B$ – see e.g. [14] –:

$$S^{BT}(O) = S_{NN}(O) = \varrho_0 \chi_T k_B T + \delta^2 S_{CC}(O), \quad (7)$$

where

χ_T = isothermal compressibility,
k_B = Boltzmann constant,
T = absolute temperature,
δ = $(\partial V_M/\partial c_A)/V_m$ = dilatation factor,
V_M = molar volume.

Experimental procedure and data reduction

Four Cs-Sb specimens containing 15, 25, 35, and 50 at% Sb were prepared. The neutron diffraction experiments were performed with the powder diffractometer D4 at the high flux reactor of the Laue-Langevin-Institute, Grenoble. The construction of the vanadium sample-containers, the diffraction runs, and the data correction for background, absorption, container contribution, and multiple scattering were done in the same way as described in previous papers [8, 15]. The normalization of the corrected scattering intensity according to Krogh Moe [16] yielded the coherently scattered intensity per atom $I_C(Q)$ and finally the total structure factor

Table 1. Scattering- and absorption-parameters for neutrons: b = coherent scattering length, σ^{inc} = incoherent scattering cross section, σ^a = absorption cross section.

	b [10^{-12} cm]	σ^{inc} [barn]	σ^a ($\lambda = 0.692$ Å) [barn]
Cs	0.546 [17]	0.22 [15]	10.89 [18]
Sb	0.564 [17]	0.17 [17]	2.05 [18]

$S^{FZ}(Q)$ using (1). The scattering- and the absorption-parameters used in the present study for Cs and Sb are listed in Table 1. The densities of the Cs-Sb melts were taken from Ref. [19] and are listed in Table 2.

Results and discussion

Structure factors

The structure factors $S^{FZ}(Q)$ of the four Cs-Sb alloys are plotted in Fig. 1 together with that of pure Cs, taken from [15], and that of pure Sb, taken from [20]. They have been obtained by smoothing the experimental data with a cubic spline fit method [21]. In Table 2 some characteristic figures of the structure factors are compiled.

Proceeding from pure Cs to $Cs_{75}Sb_{25}$ in Fig. 1, one observes a shift of the position of the main peak which, however, from 25 at% Sb up to 50 at% Sb does not change.

There are two very interesting features, namely:

i) With $Cs_{85}Sb_{15}$ and also with $Cs_{75}Sb_{25}$ a pronounced rise of $S(Q)$ versus small Q-values, i.e., a small angle scattering effect is observed, and
ii) an additional peak at $Q^a = 0.95$ Å^{-1} in front of the main maximum exists which increases going from $Cs_{75}Sb_{25}$ to $Cs_{50}Sb_{50}$.

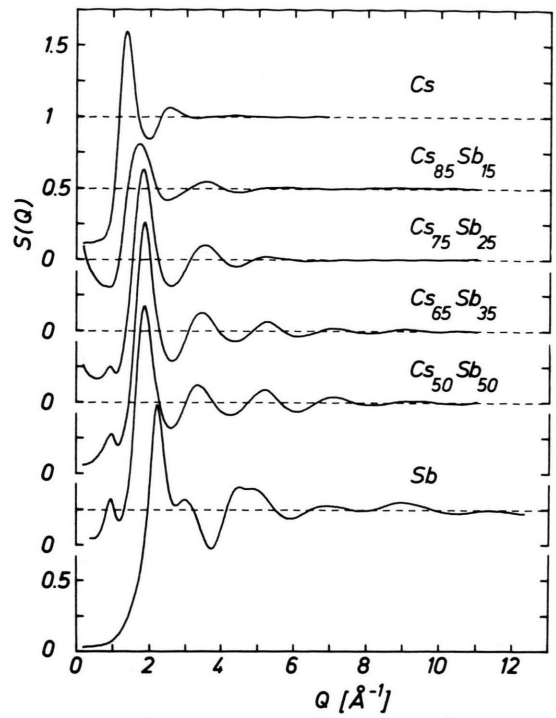

Fig. 1. Total Faber Ziman structure factors $S(Q)$.

The discussion of both scattering effects can be done by means of (6) and (7): For the alloys containing 15 at% Sb and 50 at% Sb, respectively, (6) is written as:

$$\begin{aligned} S^{BT}(Q)/_{15\text{ at\% Sb}} &= 1.00\, S_{NN}(Q) + 0.0016\, S_{CC}(Q) \\ &\quad + 0.081\, S_{NC}(Q)\,, \\ S^{BT}(Q)/_{50\text{ at\% Sb}} &= 1.00\, S_{NN}(Q) + 0.0016\, S_{CC}(Q) \\ &\quad + 0.080\, S_{NC}(Q)\,. \end{aligned} \tag{8}$$

One can see that due to the very small difference of the scattering lengths of Cs and Sb, the total struc-

Table 2. Structural parameters of liquid Cs-Sb alloys. $S(Q^I)$ = height of the structure factor at the position of the main peak Q^I. Q^a = position of the additional peak, $R^{n,m}$ = m-th subpeak of the n-th coordination shell, N^I = coordination number (*: the value $N^I = 5.6$ in Ref. [20] was calculated using the tangent-method), R_i^I, R_0^I = integration limits for the calculation of N^I.

Sample	Temperature [°C]	Density [g/cm^3]	Q^I [Å^{-1}]	$S(Q^I)$	Q^a [Å^{-1}]	$R^{I,1}$ [Å]	$R^{I,2}$ [Å]	$R^{II,1}$ [Å]	$R^{II,2}$ [Å]	$R^{II,3}$ [Å]	N^I [Å]	R_i^I [Å]	R_0^I [Å]
Cs	600	1.51	1.36	1.59	–	5.51		10.45			10.2	3.52	7.08
$Cs_{85}Sb_{15}$	700	2.13	1.71	1.31	–	4.15	5.2	–			–	–	–
$Cs_{75}Sb_{25}$	750	3.09	1.83	1.63	0.94	4.01		7.75			8.3	3.06	5.16
$Cs_{65}Sb_{35}$	700	3.67	1.87	1.76	0.97	3.88	5.1	6.4	7.53	8.3	10.6	3.20	5.40
$Cs_{50}Sb_{50}$	600	4.38	1.86	1.67	0.95	3.95	4.7	6.4	7.57	8.2	12.1	3.24	5.38
Sb	650	6.53	2.18	1.73	–	2.95		6.37			4.6*	2.44	3.40

ture factor $S^{BT}(Q)$ is a direct measure of the correlations between density fluctuations $S_{NN}(Q)$, whereas the influence of $S_{CC}(Q)$ and $S_{NC}(Q)$ can be neglected. That means that the small angle scattering effect as well as the additional peak in Fig. 1 belong to the partial structure factor $S_{NN}(Q)$. The small angle scattering with $Cs_{85}Sb_{15}$ clearly shows that the molten alloys up to 25 at% Sb are not homogeneous, but exhibit some segregation tendency into two phases with pronounced difference of the scattering length density. Equation (7) shows how $S_{CC}(Q)$ contributes to $S_{NN}(Q)$ at small Q-values with the weight factor δ^2. From the densities of Cs-Sb alloys reported in [19] we calculated for 15 at% Sb $\delta^2 \approx 10$ which is in fact very large, and thus explains that even for the case of equal scattering lengths of both components the contribution of $S_{CC}(Q)$ to the small angle scattering in (7) is considerable.

Keeping in mind that the scattering lengths of Cs and Sb are almost equal, the occurrence of the additional maximum in Fig. 1 for $0.25 \leqq c_{Sb} \leqq 0.50$ is rather surprising. Metallic alloy systems investigated up to now, which belong to the strong-compound forming class like Au-Cs [8], Li-Pb [22], and Mg-Bi [23], exhibit a so-called "prepeak" in their structure factors which clearly could be attributed to the partial structure factor $S_{CC}(Q)$ describing the chemical short range ordering (CSRO). The additional peak displayed in Fig. 1, however, belongs to the partial structure factor $S_{NN}(Q)$ which describes the topological short range order (TSRO), and we therefore cannot describe this peak as "prepeak".

This observation is in contrast to simple chemical ordering effects in the alloys mentioned above, where ionic forces are supposed to cause a rather extended alternating arrangement of both ionic species. The occurrence of an additional peak at $S_{NN}(Q)$, on the other hand, suggests rather a molecular model for the short range order than a purely ionic model.

Therefore we may conclude that in the Cs-Sb melts containing 25 at% up to 50 at% Sb rather large stable structural units exist, the distance correlation between them being characterized by larger distances compared to the nearest neighbour distances in pure metals und thus giving rise to a scattering effect at smaller Q-values (Q^a). In this respect it must be noted that such a distance correlation between larger units only can be imagined if they are defined by rather strong chemical bonding between the atoms inside the single complexes. From the peakposition at Q^a the mean distance R^a between the molecular units can be estimated if one assumes that the scattering contribution I^a of the distance correlation at R^a to the total structure factor can be simply written as

$$I^a(Q) \sim \sin(Q\,R^a)/Q\,R^a\,,$$

which shows a first maximum at $Q^a R^a = 7.73$ from which follows: $R^a = 7.73/0.95\ \text{Å} \approx 8\ \text{Å}$. From our experience, distance correlations estimated in this way agree within 5% with the corresponding correct values.

In this connection we note that in principle correlations at larger distances may either represent intra- or intermolecular distances. For the case of intramolecular distances the correlation does not extend beyond the single molecules and the corresponding scattering effect can be well described by the expression for $I^a(Q)$ given above.

Intermolecular distance correlations on the other hand may be rather extended. In this case the expression for $I^a(Q)$ represents only a rough estimation of the value of R^a but by no means a quantitative description of the shape of the corresponding scattering contribution. From the width, $\Delta Q^a \approx 0.25\ \text{Å}^{-1}$, of the peak at Q^a the range ξ^a to which the correlations extend is estimated as $\xi^a \approx 25\ \text{Å}$ using the Scherrer formula

$$\xi^a = 2\pi/\Delta Q^a.$$

From the large value of ξ^a we conclude that the $R^a \approx 8\ \text{Å}$ represents an intermolecular distance correlation which is extended even beyond neighbouring molecular units.

Thus we arrive to the conclusion that the structure of melts from the Cs-Sb system in the concentration range $25 \leqq c_{Sb} \leqq 0.50$ can be described in an analogous manner as the structure of molten Rb_6O or of molten $Li(ND_3)_x$ ($4 \leqq x \leqq 6$) as was shown in [24].

Pair correlation functions

From the structure factors the pair correlation functions $G(R)$ were calculated using (2) and are plotted in Figure 2. The various interatomic distances and the coordination numbers extracted from these functions are listed in Table 2. The positions

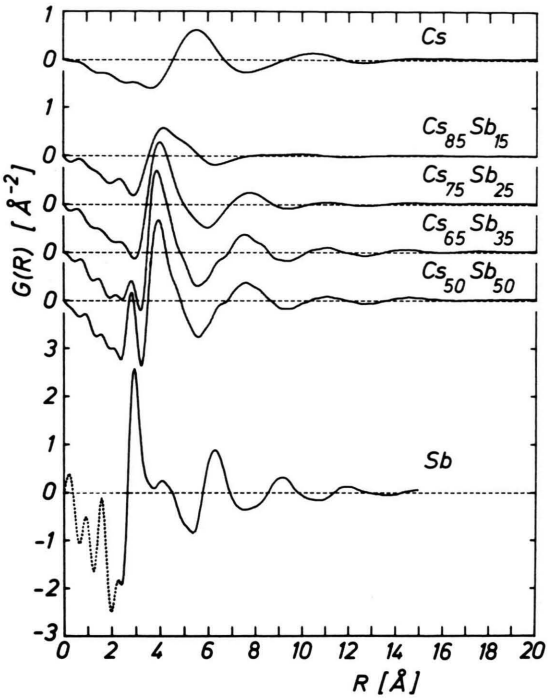

Fig. 2. Total pair correlation functions $G(R)$.

of peaks displayed as a shoulder in the total $G(R)$ had to be estimated.

The shape of the $G(R)$ curve for the $Cs_{85}Sb_{15}$ alloy supports the view that within the concentration range $0 < c_{Sb} < 25$ at% a segregation tendency is present in the alloys: The first maximum shows a double peak structure with a maximum at the position where the $Cs_{75}Sb_{25}$-curve has its main peak and a shoulder at a larger R-value which approximately corresponds to the nearest neighbour distance in pure Cs. At higher R-values the $Cs_{85}Sb_{15}$-curve exhibits nearly no structure. This fact is explained by a phase shift between the contributions from regions with small atomic distances and those from regions with large atomic distances. From these observations we conclude that within the concentration range below 25 at% Sb microsegregation between a stable $Cs_{75}Sb_{25}$ compound and excess Cs takes place. From the Q-range up to $0.7\,Å^{-1}$ in which the small angle scattering effect occurs in Fig. 1, the extension of the inhomogeneities in the alloys can be roughly estimated to be of the order of several 10 Å.

The existence of strong nonmetallic bonding in liquid $Cs_{75}Sb_{25}$ is well established by the electronic properties, especially by the drastic drop of the electrical conductivity at this composition (see Ref. [11]). In this respect comparison of the structural results with those of the corresponding crystalline phase is worthwhile. The intermetallic compound Cs_3Sb has the highest melting point (725 °C) in the Cs-Sb system. It is well known to be an intrinsic semiconductor and, based on a structural investigation [25], covalent-ionic mixture of bonding has been suggested. The structure can be described by two interpenetrating diamond lattices where both kinds of atoms have 8 nearest neighbours at a distance of 3.96 Å. This distance agrees well with the nearest neighbour distance $R^1 = 4.01$ Å in liquid $Cs_{75}Sb_{25}$. Concerning the coordination number $N^1 = 8.3$, the following considerations are necessary: For the case of equal scattering lengths ($b_{Cs} = b_{Sb}$) and using the relationship $c_{Cs}\,\varrho_{CsSb} = c_{Sb}\,\varrho_{SbCs}$ (3) is written as:

$$\varrho(R) = c_{Cs}\,\varrho_{Cs}(R) + c_{Sb}\,\varrho_{Sb}(R)\,, \tag{9}$$

with

$$\varrho_{Cs}(R) = \varrho_{CsCs}(R) + \varrho_{CsSb}(R)\,,$$
$$\varrho_{Sb}(R) = \varrho_{SbSb}(R) + \varrho_{SbCs}(R)\,.$$

Comparison of the nearest neighbourhood in liquid and solid $Cs_{75}Sb_{25}$ makes only sense if we assume the number of nearest neighbours of the Cs atoms to be equal to that of the Sb atoms also in the liquid alloy. This so-called Keating condition [26] requires at least equal sizes of both atomic species. The shift of the main peak of $G(R)$ in Fig. 2 to a smaller R-value, going from pure Cs to $Cs_{75}Sb_{25}$, clearly illustrates that in $Cs_{75}Sb_{25}$ cesium cannot be present in a metallic type state with its large atomic diameter (5.51 Å), but with an appreciably smaller diameter. Therefore the assumption that the sizes of both components in this alloy are not very different seems to be reasonable, keeping in mind that otherwise the $G(R)$ curve would show a splitting of the main maximum or at least a rather large width. The Keating condition is written as:

$$\varrho(R) = \varrho_{Cs}(R) = \varrho_{Sb}(R)\,,$$

where R hereby means the range of the first coordination shell. Summarizing these considerations we state that the value $N^1 = 8.3$ calculated with (4) from $\varrho(R)$ represents a real coordination number which is in good agreement with the corresponding value in crystalline Cs_3Sb.

In addition it is interesting to state that for a predominantly ionic bonding scheme with the forma-

tion of Cs^+ and Sb^{3-} ions in the liquid compound Cs_3Sb a nearest neighbour distance of $r_{Cs^+} + r_{Sb^{3-}} = (1.67 + 2.45)$ Å = 4.12 Å would be expected. This is not consistent with the value observed here for $R^{I,1}$ which ranges from 3.9 to 4.0 Å – see table 2.

In the following the results for $Cs_{65}Sb_{35}$ and $Cs_{50}Sb_{50}$ will be discussed. From the fact that the position of the main peak at $R^{I,1}$ does not change significantly compared to that of $Cs_{75}Sb_{25}$ one may conclude that some structural properties of $Cs_{75}Sb_{25}$ are preserved when the Sb concentration is increased. Nevertheless one observes a change of the $G(R)$ curves in Fig. 2 with increasing Sb content: An additional peak at $R^c = 2.83 - 2.84$ Å occurs whose amplitude is larger for $Cs_{50}Sb_{50}$ than for $Cs_{65}Sb_{35}$. Furthermore these two alloys exhibit a shoulder at the right hand side of their main peak and detailed poorly resolved structure in the region of the second maximum at R^{II}. These features reflect a rather complex structure of both alloys which is clearly different from that of the so-called "normal" liquid metallic alloys.

The atomic distance at R^c is smaller than the nearest neighbour distance in pure molten Sb (2.99 Å), but is in accordance with the diameter of covalently bonded Sb. Therefore this peak is attributed to the partial pair distribution function $\varrho_{SbSb}(R)$. Neglecting the contributions of the other partial distribution functions in this R-range, the partial coordination number Z_{SbSb} can be calculated from this part of $\varrho(R)$ and we obtain $Z_{SbSb} = 2$ for the case of $Cs_{50}Sb_{50}$. The width of the peak at R^c is obtained as $\Delta R^c/R^c = 13\%$, after taking the broadening due to the limited Q-range in the Fourier transformation into account. This very small peak width shows that the bond length between a central Sb atom and its two Sb neighbours is well defined.

Finally we should point out that the value of $R^c = 2.84$ Å is directly comparable with the covalently bonded Sb-Sb-distance of 2.85 Å [27] of the corresponding solid compound semiconductor CsSb. The crystal structure of this compound [27] is orthorhombic, isotypic with the NaP-structure and is characterized by spiral Sb-chains parallel to the b-axis. Thus we have to conclude based on the coordination number $Z_{SbSb} = 2$ and the agreement in the bond length that in both solid and liquid CsSb very similar chemical bonding exists, i.e. covalently bonded Sb-chain units.

This covalent bonding obviously leads to the formation of rather stable – see also [28] – large structural units in the melt with long range spatial correlations between them giving rise to the scattering peak in the structure factor at Q^a. The average distance $R^a \approx 8$ Å between the molecular units which was estimated from Q^a above falls within the range of the second maximum of $G(R)$ and might be identified with the subpeak $R^{II,3}$.

The shoulder at $R^{II,1}$ corresponds to the position of the second maximum of the $G(R)$-curve of pure Sb at 6.37 Å.

Detailed discussion, however, of the origin of the subpeaks of the second maximum and the shoulder on the right hand side of the main maximum would require the knowledge of the three partial distribution functions. It should be mentioned, however, that, due to the lack of suitable stable isotopes of Cs and Sb, the experimental determination of partial structure factors with the isotopic substitution method is not feasible for the Cs-Sb-system.

Summarizing the results of the present study we state that the atomic scale structure of liquid Cs-Sb alloys deviates significantly from that of metallic alloys. The accordance of structural features with those of respective solid compounds Cs_3Sb and CsSb suggests similar characteristics of chemical bonding in the solid and in the liquid state at corresponding compositions. Therefore a predominantly ionic model can be excluded on the basis of these results.

Acknowledgements

Thanks are due to the Institute Laue-Langevin, Grenoble for the allocation of beam time at the high flux reactor and to the Deutsche Forschungsgemeinschaft, Bad Godesberg, for financial support.

[1] R. W. Schmutzler, H. Hoshino, R. Fischer, and F. Hensel, Ber. Bunsenges. Phys. Chem. **80,** 107 (1976).
[2] J. E. Enderby, J. de Physique **35,** C4, 309 (1974).
[3] J. E. Enderby and E. W. Collings, J. Non-cryst. Solids **4,** 161 (1970).
[4] M. Cutler, Liquid Semiconductors, Academic Press, London 1977.
[5] F. Hensel, Adv. Phys. **28,** 555 (1979).
[6] J. E. Enderby, in "Amorphous and Liquid Semiconductors", (ed. J. Tauc), Plenum Press (1974).
[7] W. Freyland and G. Steinleitner, Inst. Phys. Conf. Ser. No. **30,** 488 (1977).
[8] W. Martin, W. Freyland, P. Lamparter, and S. Steeb, Phys. Chem. Liq. **10,** 61 (1980).
[9] R. Evans and M. M. Telo da Gama, Phil. Mag. **B41,** 351 (1980).
[10] C. Holzhey, F. Brouers, and J. R. Franz, J. Phys. **F11,** 1047 (1981).
[11] H. Redslob, G. Steinleitner, and W. Freyland, Z. Naturforsch. **27 a,** 587 (1982).
[12] C. N. J. Wagner, J. Non-cryst. Solids **31,** 1 (1978).
[13] T. E. Faber and J. M. Ziman, Phil. Mag. **11,** 153 (1965).
[14] A. B. Bhatia and D. E. Thornton, Phys. Rev. **B 2,** 3004 (1970).
[15] W. Martin, W. Freyland, P. Lamparter, and S. Steeb, Phys. Chem. Liq. **10,** 49 (1980).
[16] J. Krogh Moe, Acta Cryst. **9,** 951 (1956).
[17] L. Koester, in "Neutron Physics", Springer Tracts in Modern Physics **80,** 1 (1977).
[18] G. E. Bacon, Neutron Diffraction, 3rd ed., Clarendon Press, Oxford 1975.
[19] See Ref. [11], and: A. Kempf and W. Freyland, private communication.
[20] P. Lamparter, S. Steeb, and W. Knoll, Z. Naturforsch. **31 a,** 90 (1976).
[21] M. D. J. Powell, in "Curve Fitting by cubic splines", Report T. P. 307 (1967).
[22] H. Ruppersberg and H. Egger, J. Chem. Phys. **63,** 4059 (1975).
[23] M. Weber, S. Steeb, and P. Lamparter, Z. Naturforsch. **34 a,** 1398 (1979).
[24] P. Chieux and H. Ruppersberg, J. de Physique **41,** 145 (1980).
[25] K. H. Jack and M. M. Wachtel, Proc. Roy. Soc. London **A 239,** 46 (1957).
[26] D. T. Keating, J. Appl. Phys. **34,** 923 (1963).
[27] H. G. von Schnering, W. Hönle, and G. Krogull, Z. Naturforsch. **34 b,** 1678 (1979).
[28] D. J. Kirby, R. Dupree, and W. Freyland, Phil. Mag. (1982), in press.